Application of TLR agonists in cancer immunotherapy: from late to early, from systemic to local

Koster, B.D.

2020

document version
Publisher's PDF, also known as Version of record

Chapter 6

T cell infiltration upon local CpG-B delivery in early-stage melanoma is predominantly related to CLEC9A^{+}CD141^{+} cDC1 and CD14^{+} antigen-presenting cell recruitment

Manuscript in preparation

Bas D. Koster
Marta López González
Mari F.C.M. van den Hout
Annelies W. Turksma
Berbel J.R. Sluijter
Barbara G. Molenkamp
Paul A.M. van Leeuwen
Pepijn G.J.T.B. Wijnands
Saskia Vosslamber
Rik J. Scheper
Alfons J.M. van den Eertwegh
M. Petrousjka van den Tol
Ekaterina S. Jordanova
Tanja D. de Gruijl

Abstract

Background: We previously reported CpG-B injection at the primary tumor excision site one week before re-excision and sentinel node biopsy (SNB) to result in enhanced immune activation of the sentinel lymph node (SLN), increased melanoma specific $CD8^+$ T cell rates in the peripheral blood, and prolonged recurrence-free survival. Here, we assessed recruitment and activation of antigen-presenting cell (APC) subsets at the injection site in relation to APC recruitment in the SLN and T cell infiltration.

Methods: Re-excision skin specimens from patients with clinical stage I-II melanoma, collected seven days after intradermal injection of either saline (n=10) or 8 mg CpG-B (CPG7909, n=12), were examined by immunohistochemistry, quantifying immune subsets in the epidermis, papillary, and reticular dermis. Obtained counts were related to flowcytometric data from matched SLN samples. Additional *in vitro* cultures and transcriptional analyses on peripheral blood mononuclear cells (PBMC) were performed to ascertain CpG-induced APC activation and chemokine profiles.

Results: Significant increases in $CD83^+$, $CD14^+$, $CD68^+$, and $CD123^+$ APC were observed in the reticular dermis of CpG-injected skin samples. Fluorescent double or triple staining revealed recruitment of both $CD123^+BDCA2^+$ plasmacytoid dendritic cells (pDC) and $BDCA3/CD141^+CLEC9A^+$ type-1 conventional DC (cDC1), of which only the cDC1 showed considerable levels of CD83 expression, a clear sign of activation. Simultaneous CpG-induced increases in T cell infiltration were strongly correlated with both cDC1 and CD14 counts. Moreover, cDC1 and $CD14^+$ APC rates in the reticular dermis and matched SLN suspensions were positively correlated. Flowcytometric, transcriptional, and chemokine release analyses of PBMC, upon *in vitro* or *in vivo* exposure to CpG-B, indicate a role for the activation and recruitment of both cDC1 and $CD14^+$ monocyte-derived APC in the release of CXCL10 and subsequent T cell infiltration.

Conclusion: The CpG-B-induced concerted recruitment of cDC1 and $CD14^+$ APC to the injection site and its draining lymph nodes, will allow for both the (cross-)priming of T cells and their subsequent homing to effector sites.

Introduction

Conventional dendritic cells (cDC) in the healthy skin are capable of capturing and processing antigens before migrating to the regional lymph nodes where they can elicit an immune response by stimulating antigen specific T cells (1). Langerhans Cells, with high expression levels of CD1a and Langerin, are mainly found in the epidermis whereas $CD1c^+$ dermal DC are found in the dermis of healthy steady-state skin. A third, low-frequent skin cDC subset, also found in the dermis, is the BDCA3/$CD141^+$ DC population. This subset, designated cDC1, is superior at cross-presenting antigens and expresses relatively high levels of the C-type lectin receptor CLEC9A (2). Besides cDC, a $CD14^+$ macrophage-like APC subset represents a large part of the APC that are found in healthy skin (1). Compared to cDC, these macrophage-like cells have a rapid turn-over and poor antigen presenting and migrating capabilities, but serve a role in the boosting and maintenance of (tissue-resident) memory T cells (3). In inflamed skin, another class of DC called plasmacytoid dendritic cells (pDC) can be found (4). Even though these are relatively weak T effector cell primers (5), pDC elicit a powerful immune response by producing large amounts of typ- I interferons (IFN-I), like IFNα and IFNβ, upon activation, which in turn can activate cDC, $CD8^+$ effector T cells, and NK cells. In addition, inflammation can lead to the recruitment and local differentiation of monocyte-derived APC subsets.

In melanoma patients, DC development and activation is hampered in the tumor microenvironment (TME) due to the local release of soluble mediators such as IL-10, prostaglandins, VEGF, IL-6, and TGFβ (6). We recently also demonstrated a role for hampered DC activation in the first-line melanoma-draining lymph node, the so-called sentinel lymph node (SLN) in early immune escape (7). This inhibited DC development and activation not only hampers T cell priming, but also blocks effector T cell recruitment to the TME, thus effectively interfering with the efficacy of both immune checkpoint blockade and (*in vivo*) vaccination approaches. DC express Toll like receptors (TLR) that can recognize molecular patterns from pathogens. Leading to their activation. TLR-L have been clinically explored, both as vaccine adjuvants and as intratumorally applied immune modulators, aiming at DC recruitment and activation in the TME, thus ameliorating tumor-related immune suppression and facilitating effector T cell (cross-)priming and recruitment. Unlike cDC, human pDC express TLR9 that binds unmethylated Cytosine-phosphate-Guanine (CpG) oligodeoxynucleotides (ODN) (8). CPG7909 is a synthetic B-class CpG (CpG-B) that activates both B cells and pDC and leads to

the release of type-I IFN (9,10). We previously reported on two phase II clinical trials, in which patients with clinical stage I-II melanoma received intradermal (i.d.) injections with either CPG 7909 or plain saline in the week leading up to a sentinel node biopsy (SNB) and a re-excision of the primary tumor excision scar. We found that this local i.d. administration of CpG-B resulted in activation of both lymph node resident (LNR-) cDC and pDC subsets in the SLN (11), elevated frequencies of tumor-specific T cells in the peripheral blood (12), lower rates of tumor-positive SLN, and even an increased recurrence-free survival (RFS), as compared to the administration of a saline placebo in the control group (13).

Here, we set out to study the local effects of i.d. CpG-B injection at the primary tumor re-excision site in terms of APC subset recruitment and activation. We related our findings to DC subset content of matched SLN samples as well as to T cell infiltration, in order to gain further insight in the loco-regional events leading up to T cell activation and recruitment, and, eventually, to systemic tumor control.

Materials and Methods

Patients

This study made use of clinical materials and immune monitoring data collected over the course of two consecutive single-center, single-blinded, randomized, and placebo-controlled phase II clinical trials, conducted between June 2004 and June 2007 at the VU University Medical Center in Amsterdam, The Netherlands (ISRCTN63321797). Enrolled patients were diagnosed with clinical stage I-II melanoma according to criteria of the American Joint Committee on Cancer and were scheduled to undergo SNB. They were randomly assigned to receive preoperative local administration of either CpG-B (PF-3512676; Coley Pharmaceutical Group, Wellesley, MA) or saline (NaCl 0.9%) adjacent to the excision scar of the primary tumor, in the week leading up to re-excision and SNB. Inclusion and exclusion criteria were as described previously (13,14). Prior to routine diagnostic procedures, excised SLN were bisected and viable cells were scraped from the cutting surface, washed, counted, and further processed as previously described (14). The studies were approved by the Institutional Review

Board of the VU University Medical Center and written informed consent was obtained from each patient before treatment in accordance with the Declaration of Helsinki.

Immunohistochemistry studies

23 patients were randomly assigned to receive one preoperative i.d. injection of either 8 mg CpG-B dissolved in 1.6 ml saline (NaCl 0.9%; n = 11), or 1.6 ml plain saline alone (n = 12) seven days before the re-excision and SNB (11). One patient, who received CpG-B, was excluded from our analyses because the patient did not undergo re-excision. The excision margin was 1 cm for melanomas with a Breslow thickness of ≤ 2 mm and 2 cm for lesions ≥ 2 mm. See Table I for an overview of these patients' clinical characteristics.

Transcriptional analyses

19 patients were randomly assigned to receive 4-ml i.d. injections of either 1 mg CpG-B (n=10) or of saline (n=9), 7 and 2 days before re-excision and SNB. Viable peripheral blood mononuclear cells (PBMC) were isolated prior to the injections on day -7 and prior to re-excision and SNB on day 0 and cryopreserved for further transcriptional and flowcytometric analysis as previously described (15).

Table 1: Patient characteristics.

Characteristic	Total		CpG-B		Saline	
	n	*%*	*n*	*%*	*n*	*%*
Total	22	100	10	45	12	55
Sex						
Male	14	64	6	60	8	67
Female	8	36	4	40	4	33
Age (years)						
Range	26-75		33-75		26-71	
Mean	53,22		50,86		55,19	
Site of primary melanoma						
Trunk	12	55	6	60	6	50
Upper extremity	3	14	1	10	2	17
Lower extremity	7	31	3	30	4	33
Head/ Neck	0	0	0	0	0	0
Breslow thickness (mm)						
Median	1,55		1,42		1,6	
Mean	1,63		1,56		1,68	
Type of melanoma						
Superficial spreading	16	73	7	70	9	75
Nodular	4	18	1	10	3	25
Spitzoid	1	5	1	10	0	0
Acrolent	1	5	1	10	0	0
Clark level						
II	3	14	2	20	1	8
II-III	3	14	2	20	1	8
III	3	14	1	10	2	17
IV	13	59	5	50	8	67
Ulceration						
Absent	19	86	9	90	10	83
Present	3	14	1	10	2	17
Lymphatic invasion						
Absent	22	100	10	100	12	100
Present	0	0	0	0	0	0
Sentinel node						
positive	6	27	2	20	4	33
Negative	16	73	8	80	8	67
Inflamed aspect re-excision specimen						
Absent	14	64	4	40	10	83
Present	8	36	6	60	2	17
Melanoma found in re-excision specimen						
Absent	22	100	10	100	12	100
Present	0	0	0	0	0	0

Immunohistochemistry (IHC) of the skin

Paraffin sections (4 µm) of the re-excision skin samples of 22 patients were collected, mounted on Superfrost Plus glass slides, and dried overnight at 37°C. After deparaffination, the tissue sections were hydrated through decreasing (v/v) percentages of ethanol and endogenous peroxidase was blocked with 0,1% hydrogenperoxide in methanol. Antibodies against CD1a, CD14, CD83, (Monosan, Uden, the Netherlands), Langerin (Novocastra, Newcastle, United Kingdom), CD123, DC-SIGN (BD Pharmingen, San Jose, United States), CD3, CD68 (Dako, Heverlee, Belgium) were used. The slides were pre-treated with 10 mM TRIS, 1 mM EDTA pH 9 (CD3, CD14, CD123, DC-SIGN, CD68) or 10 mM Na-citrate pH 6 (CD1a, CD83, Langerin). Primary antibodies were applied and visualization was performed with Bondmax (Menarini Group, Malmö, Sweden) for CD3, the Power Vision plusTM system (Immunologic, Duiven, The Netherlands) for CD14, and the EnvisionTM horseradish peroxidase system (DakoCytomation, Glostrup, Denmark) for the other markers, all according the manufacturer's instructions.

IHC Quantification

All slides were coded and counted by two independent observers blinded to the patients' treatment. The number of positive cells in the epidermis, the superficial papillary dermis (stratum papillare) and the reticular dermis (stratum reticulare) were evaluated by direct counting of stained nucleated cell bodies per x400 magnification microscopic field i.e. high power field (HPF). Each observer counted 10 HPFs in the epidermis, the superficial dermis, defined as the HPF adjacent the epidermis, and the reticular dermis. Counts were calculated as the average of the independent observers and expressed as mean number of positive cells per HPF.

Double or triple immunofluorescent IHC

Paraffin sections were cut (4 µm) and dried overnight on coated slides at 37°C. After deparaffination, the tissue sections were hydrated through decreasing (v/v) percentages of

ethanol and incubated for 10 min in boiling antigen retrieval buffer EDTA. After cooling and washing, the slides were incubated overnight in a moist chamber with antibodies against BDCA2 (Miltenyi Biotec, Bergisch Gladbach, Germany, mouse IgG2a, 201A), CD123 (BD Pharmingen, San Jose, United States, mouse IgG2a, 7G3), CD83 (Monosan, mouse IgG1, 1H4B/MONX10851), BDCA3 (LifespanBiosciences, Rabbit monoclonal, LS-B7307/35332), Clec9a (R&D, Scheep IgG, AF6049). After washing, slides were incubated for 1h with isotype specific secondary antibodies: GaM IgG1 (CD83) (647, blue or 546, red), GaM IgG2a (BDCA2 or CD123) (488, green), GaR (BDCA3) (546, red) Donkey anti sheep (Clec9) (488, green). After washing, slides are covered with 1 drop of MOWIOL and with a coverslip and stored at 4°C. The slides were evaluated using a Fluorescence microscope (Axiovert-200M) at a magnification of ×100 and ×400, and pictures were taken with a sensicam camera (PCO) and Slidebook 6 reader software (Intelligent Imaging Innovations).

Flowcytometric analyses

DC subsets from PBMC or SLN single-cell suspensions, isolated and prepared as previously described (15,16), were phenotypically analyzed by four or ten color flow cytometry, with the following mAbs, which were diluted in PBS supplemented with 0.1% BSA and 0.02% NaN3, and incubated for 30 minutes at 4°C: CD11c, CD1a, CD14, PD-L1, CD16 (BD Biosciences), CD40, CD83 (Beckman Coulter), CD86, CD80 (BD Pharmingen), BDCA3 (Miltenyi Biotec), CLEC9A, CD1c, BDCA3, CD103 (Biolegend), CD83, PD-L1 (BD Horizon). After incubation, cells were washed in FACS buffer to remove excess antibodies and used for flowcytometric analyses. Flowcytometric Analyses were performed on a FACS-Calibur flow or LSR Fortessa cytometer (Becton Dickinson), equipped with Cellquest or FACSDiva data acquisition software, respectively; data were analyzed using Cellquest (BD Biosciences) or Kaluza (Beckman Coulter) analysis software.

PBMC cultures

PBMC obtained from healthy donors upon written informed consent (Sanquin Blood Supply Services, Amsterdam, The Netherlands) were plated in RPMI medium (BioWhittaker, Verviers,

Belgium) supplemented with 10% heat inactivated Fetal Calf Serum (FCS) (Hyclone Laboratories, Logan, Utah, USA), 100 I.E./ml sodium penicillin, 100 µg/ml streptomycin sulfate, 2 mM L-glutamine, and 50 µM β-mercaptoethanol, (at 5 million/ml) and cultured for 48h in the absence or presence of 5 µg/ml CPG7909. After 48h, supernatants were collected for chemokine analysis and the cells were harvested and analyzed by flowcytometry for APC subset frequencies and activation state. Additionally, $CD14^+$ cells were isolated by magnetic activated cell sorting (MACS) by the use of CD14 magnetic beads (MACS Milteny Biotec), and subsequently $CD11c^+$ cells were similarly MACS-isolated by a 2-step incubation with anti-CD11c (BD Biosciences), followed by Goat-anti-Mouse magnetic beads, both according to the manufacturer's protocols. The $CD14^+$ (monocytic) and $CD14^-CD11c^+$ (cDC enriched) populations were plated separately (at 1 million/ml) and cultured overnight, after which supernatants were collected for chemokine analysis by flowcytometric cytokine bead array analysis according to the manufacturer's instructions (BD Biosciences).

Type-I Interferon (IFN) response transcript analysis

Total RNA was isolated from PBMC and reverse transcribed as previously described (17). Forty-seven type I IFN response genes (IRGs) were selected based on significant upregulation in more than three experiments published on the Interferome database (http://www.interferome.org/). Custom-designed TaqMan®assays for each IRG were supplied by Applied Biosystems. Quantitative PCR (qPCR) analysis was performed (ServiceXS B.V., Leiden, The Netherlands) using the 96.96 BioMark™ Dynamic Array for Real-Time PCR (Fluidigm Corporation, San Francisco, CA, USA), according to the manufacturer's instructions. Thermal cycling and real-time imaging of the BioMark array was carried out on the BioMark instrument, and cycle threshold (CT) values were extracted using BioMark Real-Time PCR analysis software. Relative quantities were calculated using the standard curve method, with glyceraldehyde-3-phosphate dehydrogenase (GAPDH) as a housekeeping gene. Expression levels were ^{2}log-transformed. An overall IRG score was determined by averaging the relative expression levels of all 47 IRG. Comparison of IRG expression between time points was assessed using paired t tests.

Statistical analysis

Differences in measured immune parameters between patient study groups or time points were analyzed using the two-sample Mann-Whitney U test, the Fisher's Exact test, or a two-sided Student's t-test. -sided paired Student t test was used for comparisons between 2 samples. Correlations were determined by use of the Pearson r test. Microsoft Excel (version 2010) and GraphPad Prism (Version 6.02) were used for all graphs, tables and analyses. $P < 0.05$ was considered significant.

Results

IHC analysis of APC subsets at the CpG-B- vs. saline-injected re-excision skin site

In a two-armed randomized trial aiming at immune modulation of the SLN in early-stage melanoma, patients were treated with an i.d. injection of either 8mg CpG-B or plain saline (placebo control group) at the primary tumor re-excision site. There were no significant differences in patient and tumor characteristics at baseline or after pathological assessment of the re-excision specimens and SLN between the two patient groups (Table 1). However, routine re-excision specimens examination by a pathologist (who was blinded to the experimental treatment-arms) reported that six out of ten CpG-B injected samples had an inflamed aspect showing mononuclear immune infiltrates that could not be explained as a reaction to the suture material used after the primary melanoma excision. In contrast, in re-excision specimens of saline injected patients mostly giant cell reactions to the suture materials were reported. Of note, no melanoma cells were found in any of the 22 re-excision specimens included in this study.

IHC staining with various lineage markers revealed the frequency and distribution of various APC subsets in the skin. As shown in Figure 1, in CpG-treated skin the epidermis and superficial or papillary dermis, i.e. immediately underlying the epidermis, showed an aspect consistent with steady state, i.e. $CD1a^+Langerin^+$ Langerhans Cells (LC) located in the epidermis and scattered DC-$SIGN^+$ APC in the superficial dermis, without any sign of DC activation and migration (i.e. lack of CD83 expression in the papillary dermis). In contrast, in the reticular dermis aggregates of $CD83^+$ and $CD123^+$ cells were observed without any evidence of co-

localized DC-SIGN expression. This indicated the recruitment of DC subsets from peripheral blood, other than monocyte-derived APC, as these might be expected to express DC-SIGN. Quantification revealed no differences in APC subset markers between saline- or CpG-injected specimens in the epidermis or papillary dermis, except for a slight elevation in $CD14^+$ cells (Figure 2A and 2B). In contrast, significantly higher numbers of $CD83^+$, $CD68^+$, $CD123^+$, and $CD14^+$ cells were found in the reticular dermis of CpG-injected re-excision samples as compared to saline-injected samples (Figure 2C).

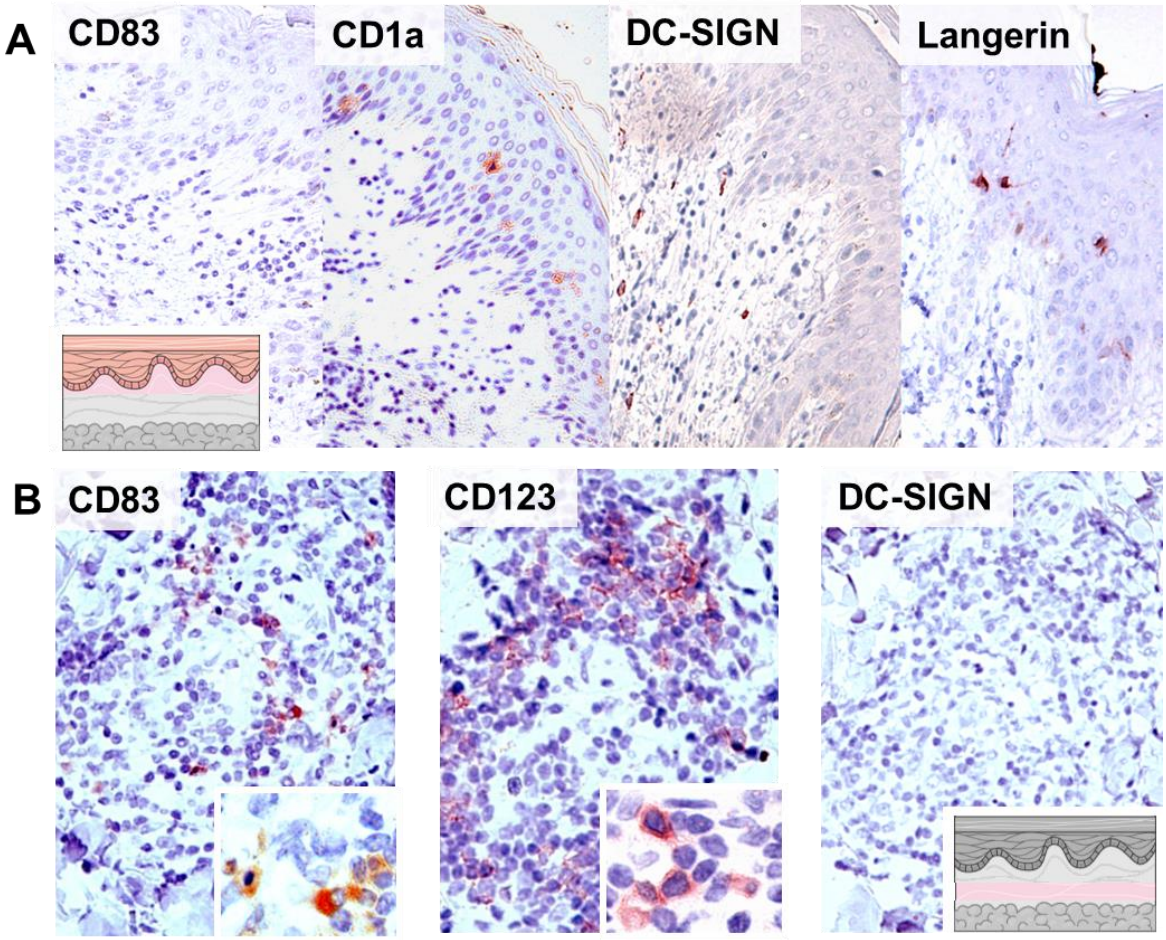

Figure 1. Immunohistochemical analysis of dendritic cell (DC) markers in CpG-B injected primary melanoma re-excision skin specimens

A) $CD1a^+$Langerin$^+$ Langerhans Cells (LC) and DC-$SIGN^+$ APC were detected in the epidermis and papillary dermis, without signs of activation (lack of CD83) or migration. **B)** In the reticular dermis, $CD123^+$ APC (pDC) and $CD83^+$ cells were observed but no DC-$SIGN^+$ APC. Schematic skin representations show epidermis+papillary dermis and reticular dermis in pink.

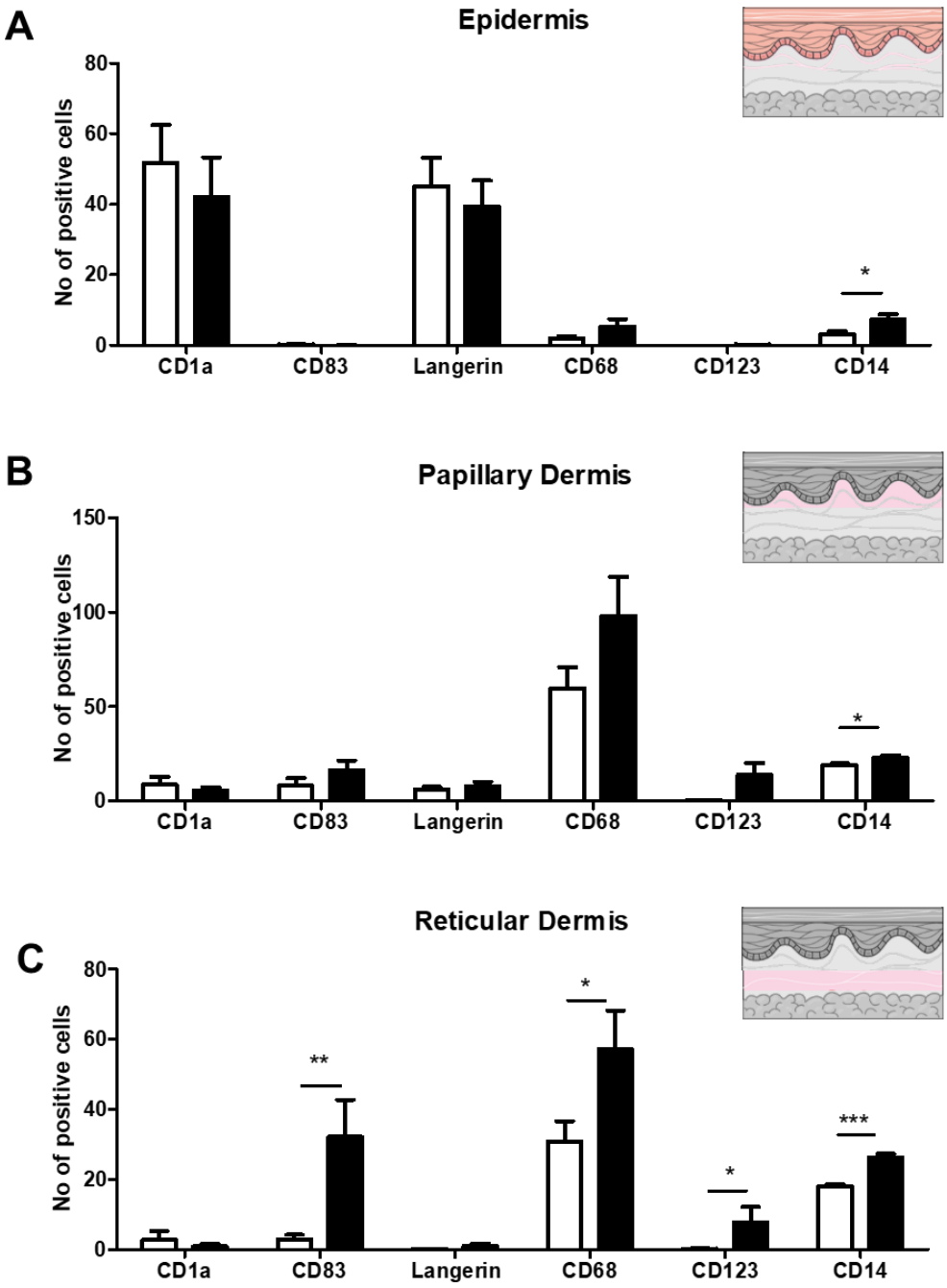

Figure 2. Immunohistochemical quantification of DC activation and subset markers in saline and CpG-injected primary melanoma re-excision specimens

In the **A)** epidermis and **B)** papillary dermis, no differences except for a slight elevation in $CD14^+$ cells was found in CpG-injected re-excision samples (closed bars) as compared to saline-injected samples (open bars). In the **C)** reticular dermis, significantly higher numbers of $CD83^+$, $CD68^+$, $CD123^+$, and $CD14^+$ cells were present in of CpG-injected re-excision samples as compared to saline-injected samples. Schematic skin representations show epidermis, papillary dermis, and reticular dermis in pink. Statistical significance: *, $P < 0.05$; **, $P < 0.01$; ***, $P < 0.001$.

Whereas the observed CD123 expression suggested pDC infiltration, CD68 and CD14 were indicative of myeloid APC infiltration. To further determine the identity of these APC recruited to the reticular dermis, we performed double and triple fluorescent IHC analyses on skin sections from CpG-administered patients (n=6). Also, two saline-injected samples were stained as negative controls. Double staining with BDCA2 (CD303) revealed the $CD123^+$ cells in CpG-injected skin to indeed be pDC (in contrast, hardly any double positive pDC were observed in saline-injected samples), but double staining with CD83 revealed these pDC to be mostly immature (Figure 3A). Triple staining demonstrated the $CD83^+$ cells in the reticular dermis to be mostly positive for CD141/BDCA3 and CLEC9A, identifying them as mature cDC1 (Figure 3B). As a positive control, a representative example of this CD83/CD141/CLEC9A triple stain on a tonsil section is shown in Supplementary Figure 1. Further quantification showed a significantly higher percentage of cDC1 to be $CD83^+$ as compared to pDC (Figure 3C) and that indeed the majority of $CD83^+$ cells in the reticular dermis consisted of cDC1 (70%, see Figure 3D).

Co-recruitment of cDC1 and CD14+ APC to the SLN and primary tumor excision site

We previously described the preferential recruitment and activation of both $CD14^-$ and $CD14^+$ LNR-cDC/APC subsets in the melanoma SLN from $CD141^+$ and $CD14^+$ blood-derived precursors upon i.d. injection of CpG-B (15). This was indeed borne out by flowcytometric analyses of available cryopreserved SLN single-cell suspensions from the same patient cohort tested by IHC for APC recruitment to the CpG- or saline-injected re-excision site (Figure 4A). Of note, we previously reported both CD141 and CLEC9A expression on LNR-cDC (15), identifying them as cDC1-like. Thus, the $CD14^-$ and $CD14^+$ LNR-cDC/APC subsets were strongly reminiscent of the respective cDC1 and CD14+ APC subsets found to be recruited to the skin upon CpG-B injection. Correlation analyses, including between matched SLN and skin samples, indeed revealed co-recruitment of $CD14^-CD83^+$ cDC1 and $CD14^+$ APC subsets to the SLN and skin/injection site (Figure 4B).

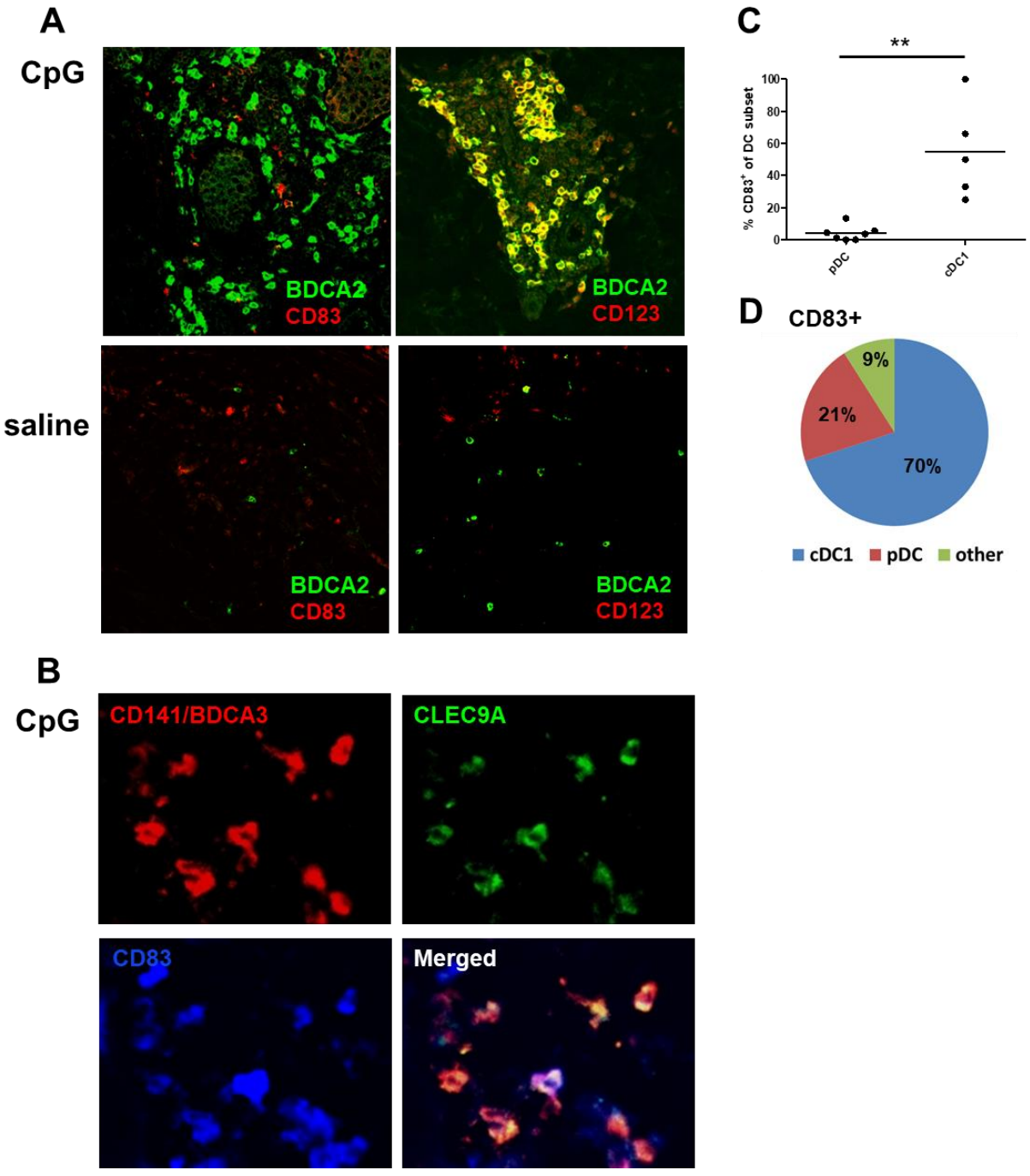

Figure 3. Phenotypic determination of CD83$^+$ APC in the reticular dermis

A) Double fluorescent immunohistochemical (IHC) analyses with BDCA2 and CD83, and BDCA2 and CD123 on skin sections from CpG-B-injected and saline-injected patients revealed the presence of mainly immature pDC only in CpG-B-injected sections. **B)** Triple fluorescent IHC analyses revealed that the CD83$^+$ cells in CpG-B injected sections were mostly positive for CD141/BDCA3 and CLEC9A, identifying them as mature cDC1. Quantification showed **C)** a significantly higher percentage of cDC1 to be CD83$^+$ as compared to pDC and **D)** that the majority (70%) of CD83$^+$ cells were indeed cDC1 in CpG-B injected sections. Statistical significance: **, $P < 0.01$.

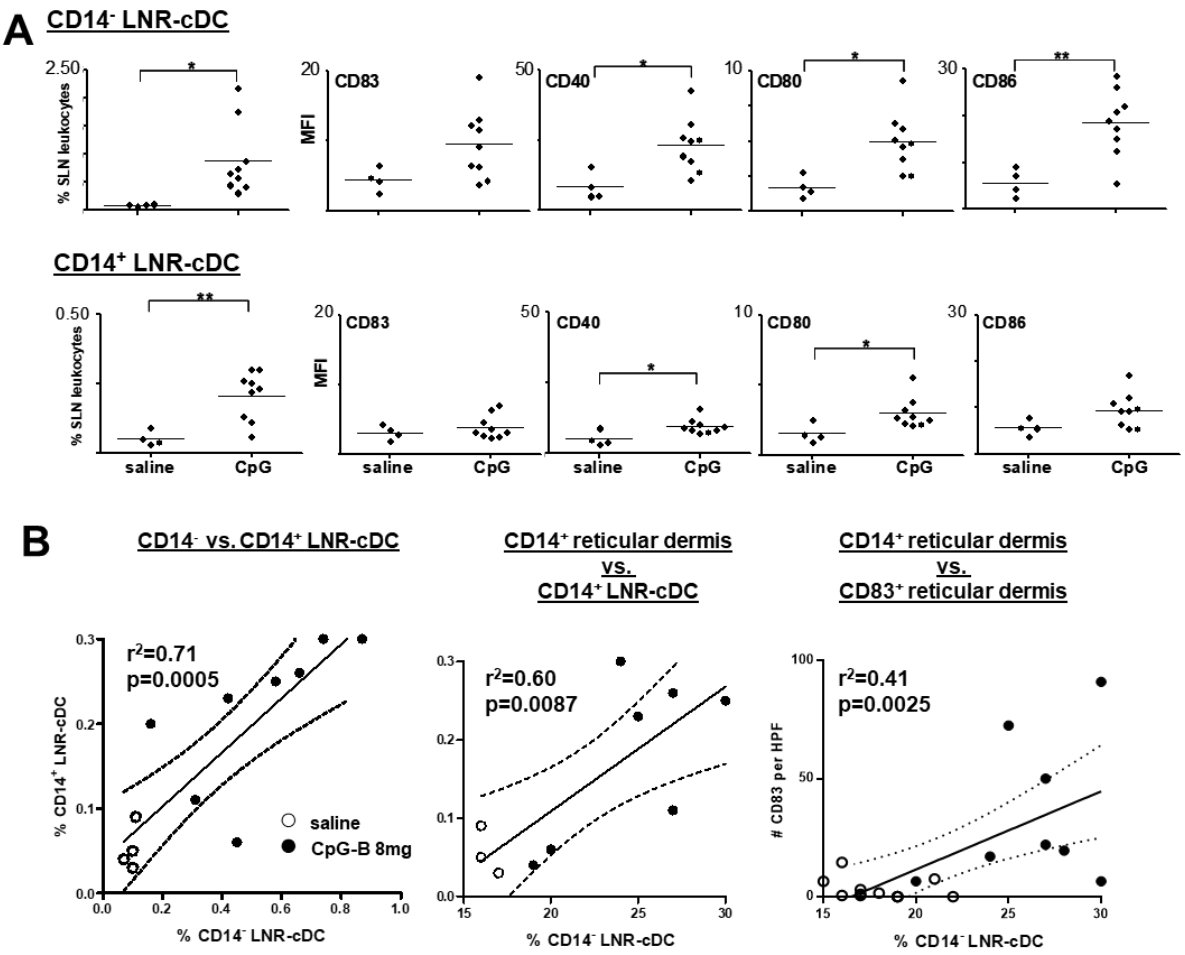

Figure 4. Flowcytometric analyses of CD14$^+$ and CD14$^-$ lymph node resident (LNR) cDC and correlations to APC subsets in matched reticular dermis

A) We found higher frequencies and activation states of CD14$^+$ and CD14$^-$ LNR cDC (by multiple markers) in CpG-B-treated patients and **B)** correlative evidence for co-recruitment of CD14$^-$CD83$^+$ cDC1 and CD14$^+$ APC subsets to the SLN and skin. Statistical significance: *, P < 0.05; **, P < 0.01.

To further ascertain their possible origins and the effects of CpG on these myeloid APC subsets, we performed 48h cultures of PBMC from healthy donors, in the presence or absence of 5 µg/ml CpG-B (CPG7909). Based on CD1c and CD141/BDCA3 expression we distinguished three cDC subsets, and based on CD16 expression, two CD14$^+$ monocytic APC subsets post-culture. Gating strategies for these myeloid cDC and monocytic APC subsets are shown in Supplementary Figure 2A. No significant differences in the distribution of these subsets between the control and CpG-B culture conditions were observed (Supplementary Figure 2B). Of the three identified cDC subsets, one (CD1c$^+$BDCA3^{dim}) did not respond to CpG exposure,

with only a significant up-regulation of CD80. In contrast, the other two subsets (i.e. $CD1c^{+}BDCA3^{+}$ and $CD1c^{-}BDCA3^{dim}$) both responded by significant up-regulation of CD83, indicating maturation induction (Figure 5). In addition, up-regulation (at varying significance levels) of CD80, PD-L1, CLEC9A, and CD103 was observed. Expression (at varying levels) of CD141/BDCA3, CLEC9A, and CD103, in all three cDC subsets, identified them as cDC1-like. In contrast, no expression of CD103 or CLEC9A was observed in the $CD14^{+}$ APC as well as low expression levels of CD83 (the latter being marginally and non-significantly up-regulated by CpG-B) (Figure 5). A remarkable up-regulation of CD16 in the monocytes was observed upon culture, indicative of a more inflammatory phenotype (Supplementary Figure 2A). In both $CD16^{-}$ and $CD16^{+}$ monocytes a significant upregulation of both CD80 and PD-L1 was observed (Figure 5).

Combined, our IHC data in skin, our flowcytometric data from matched SLN samples, and our *in vitro* culture data suggest CpG-induced activation of both mature cDC1 and more immature CD14+ APC and their co-recruitment from PB precursors to both the skin injection site and the draining SLN.

T cell infiltration in relation to recruited APC subsets

IHC analyses further revealed significantly higher numbers of $CD3^{+}$ T cells infiltrating the papillary dermis, and even more so the reticular dermis, of CpG-injected skin as compared to saline-injected skin (Figure 6A and 6B). As a growing number of studies have shown DC to be vital for the recruitment of an effector T cell infiltrate to the melanoma TME (18–21), we correlated the T cell numbers to the numbers of the different APC subsets in the reticular dermis of all tested re-excision specimens. As shown in Figure 6C, only a weak correlation with pDC numbers was observed, but a strong and significant correlation with $CD83^{+}$ (cDC1) and an even stronger and more significant correlation with $CD14^{+}$ APC numbers was found. Indeed, whereas combined CD83 and CD14 numbers showed a strong correlation to CD3 numbers infiltrating into the reticular dermis, further inclusion of pDC numbers did not add to the strength of this correlation (Figure 6D). These data suggest a dominant role for CpG-recruited cDC1 and $CD14^{+}$ APC over pDC in effecting subsequent T cell infiltration.

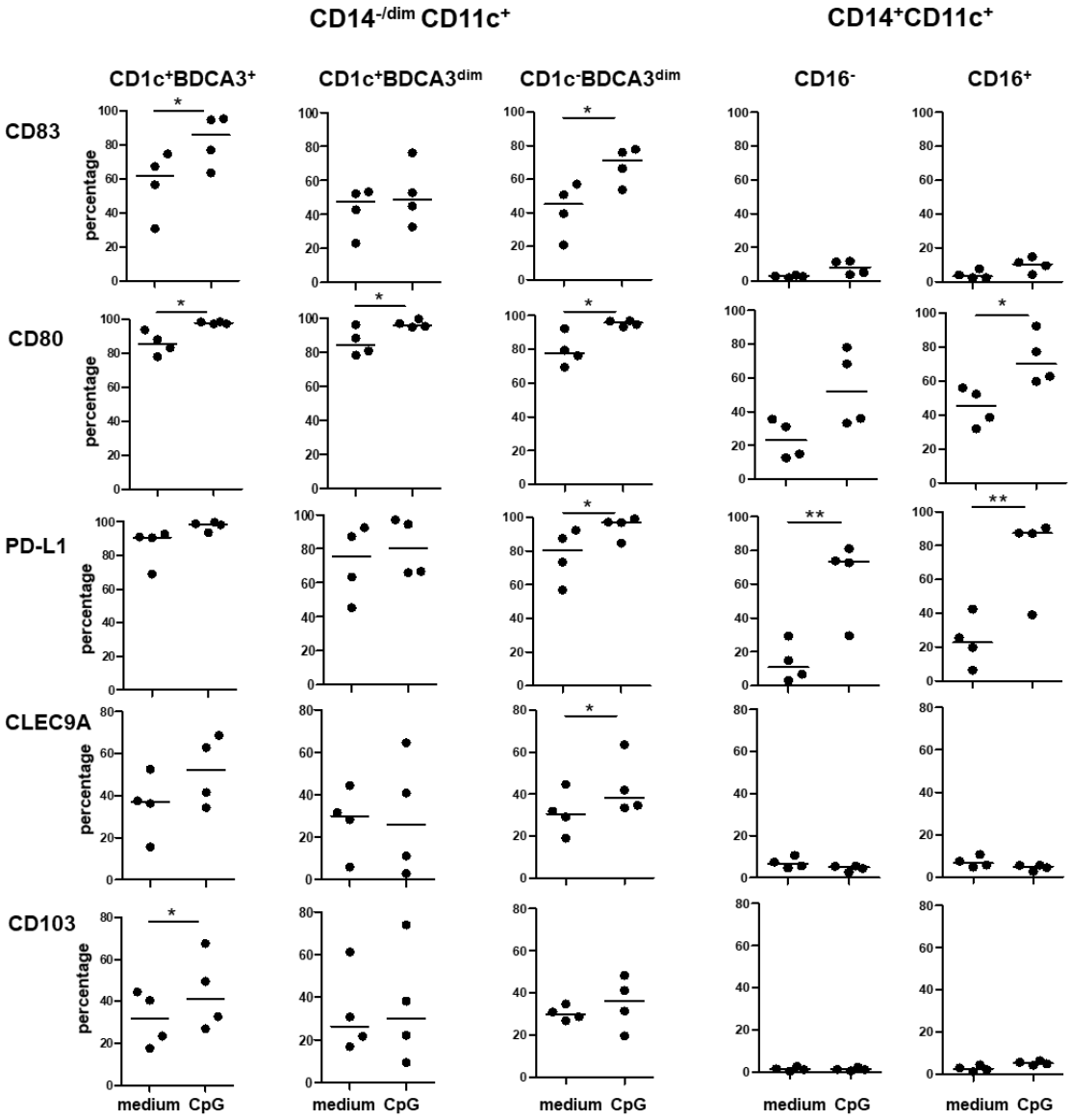

Figure 5. Flowcytometric analyses of three CD14$^{-/dim}$CD11c+ and two CD14^{+}CD11c^{+} subsets obtained from 48h control or CpG-B exposed cultures of PBMC from healthy donors

the CD1c^{+}BDCA3^{+} and CD1c^{-}BDCA3^{dim} subsets both responded to the CpG-B exposure by significant up-regulation of CD83, indicating maturation induction. Expression (of CD141/BDCA3, CLEC9A, and CD103, in all three CD14$^{-/dim}$ subsets, identified them as cDC1-like. In contrast, no expression of CD103 or CLEC9A was observed in the CD14^{+} subsets as well as low expression levels of CD83 and upregulation of only CD80 and PD-L1 upon CpG-B exposure. Statistical significance: *, $P < 0.05$; **, $P < 0.01$.

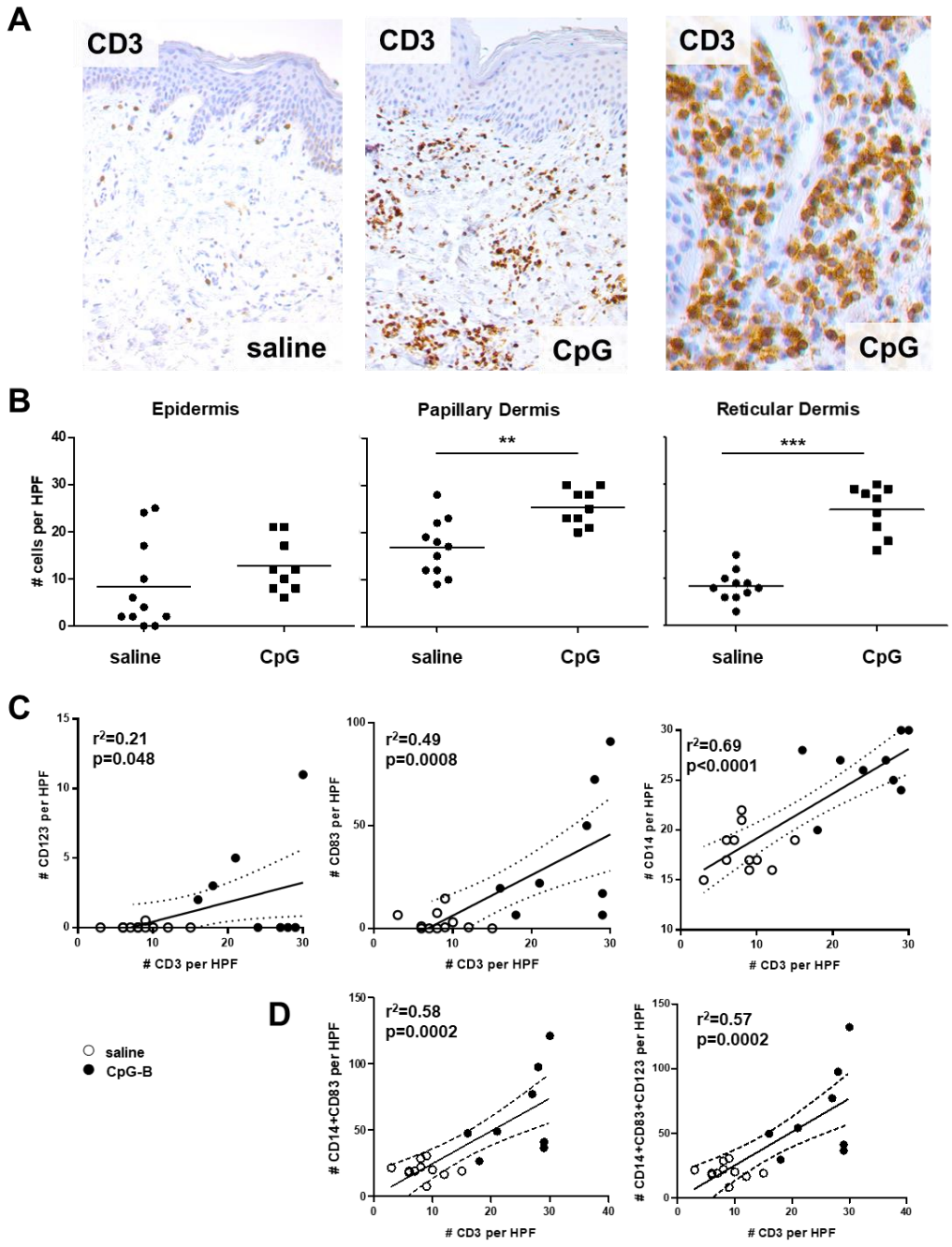

Figure 6. Dermal T cell infiltration in relation to recruited APC subsets

A) Immunohistochemical analyses revealed **B)** significantly higher numbers of $CD3^+$ T cells infiltrating the papillary dermis, and even more so the reticular dermis, of CpG-injected skin as compared to saline-injected skin. **C)** Correlation of T cell numbers to the numbers of the different APC subsets in the reticular dermis of all tested re-excision specimens show a weak correlation with pDC numbers but a strong and significant correlation with CD83+ (cDC1) and an even stronger and more significant correlation with CD14+ APC. **D)** Combined CD83 and CD14 numbers showed a strong correlation to CD3 numbers infiltrating into the reticular dermis whereas further inclusion of pDC numbers did not add to the strength of this correlation. Statistical significance: **, $P < 0.01$; ***, $P < 0.001$.

CpG-B conditioned cDC1 and CD14+ APC as a source of T cell attracting chemokines

To further substantiate a role for cDC1 and $CD14^+$ APC precursors recruited from blood for the subsequent mobilization of T cells, we assessed cDC1 activation and effector chemokine expression by transcriptional profiling of pre- and post-treatment PBMC from patients with clinical stage I/II melanoma participating in another randomized phase II clinical trial. In this trial patients received either two i.d. injections adjacent to the primary tumor excision scar of 1 mg CPG7909 or of saline, seven and two days prior to re-excision and SNB.

First we showed that this treatment regimen led to a similar co-recruitment of $CD14^-$ and $CD14^+$ LNR-cDC/APC to the SLN as in the previous patient cohort, used for the IHC studies, in which patients received one i.d. injection of 8 mg CpG or saline (see Supplementary Figure 3A). Also, by transcriptional analysis of 47 known IFN-I response genes (IRG), we showed that there was a significant induction of an IFN-I response measurable in PBMC, 7 days after the first i.d. injection of CpG-B (IRG scores, based on averaged relative IRG levels shown in Supplementary Figure 3B). Moreover, this IRG score correlated significantly with the $CD14^-$ and $CD14^+$ LNR-cDC rates in SLN (Supplementary Figure 3C), in keeping with our previous observation of a CpG-B/type-1 IFN-induced recruitment of cDC1 and $CD14^+$ APC/cDC to the SLN (15).

As the IFN-inducible transcription factor IRF8 had previously been reported as vital for terminal cDC1 differentiation (22), we determined its transcript levels and indeed found them to be significantly up-regulated post CpG-B administration (Figure 7A). As recognized IRGs CXCL10 and CXCL11 were also part of the 47 IRG signature. The transcript levels of both these effector T cell attracting chemokines were also significantly elevated after CpG-B treatment (Figure 7B and 7C). Importantly, expression levels of all three transcripts were significantly correlated to LNR-cDC frequencies (Figure 7D), indicating that the CpG-triggered IFN-I response led to cDC1 activation in conjunction with CXCL10 and CXCL11 expression. Supplementary Figure 3D shows a heat map of Pearson correlation *P* values for the IRF8 and the separate or combined CXCL10 and CXCL11 transcript levels versus the separate or combined $CD14^-$ and $CD14^+$ cDC rates in the SLN. IRF transcripts were only significantly correlated to the $CD14^-$ LNR-cDC rates, consistent with their cDC1-like state. In contrast, the

chemokine transcript levels were highly significantly correlated to the frequencies of both subsets.

To confirm CpG-induced production of effector T cell attracting chemokines by both cDC1 and $CD14^+$ APC, we determined chemokine release levels 48h after *in-vitro* PBMC exposure to CpG-B. As shown in Figure 7E, this led to elevated release levels of CXCL10, CXCL9, and CXCL11, which reached significance only in the case of CXCL10. At 48h, $CD14^+$ and $CD14^-CD11c^+$ (i.e. enriched for cDC1, see Supplementary Figure 2A) cells were sorted from the CpG-exposed PBMC cultures and put in culture separately. Supernatants were collected after overnight culture and both were found to contain variable but equally high levels of CXCL10, confirming production of this effector T cell attracting chemokine by both $CD14^+$ APC and by cDC1 (Figure 7F).

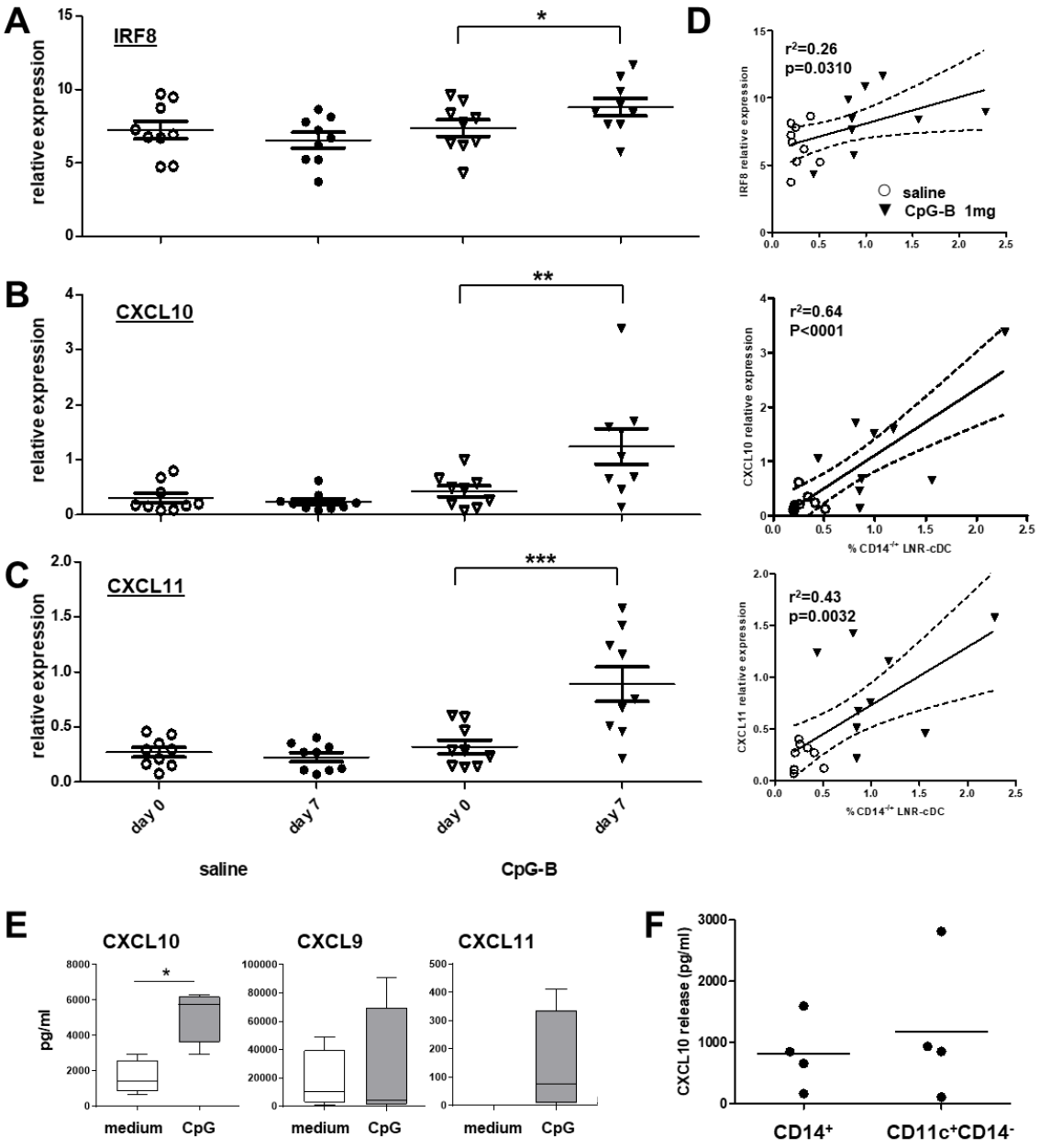

Figure 7. IRF8 and chemokine expression and release levels after CpG-B stimulation in correlation with lymph node resident DC subset frequencies

We found significantly up-regulated transcript levels of **A)** IRF8, **B)** CXCL10 and **C)** CXCL11 in PBMC from patients, seven days post CpG-B administration as compared to pre-treatment levels. **D)** Expression levels of all three transcripts were significantly correlated to LNR-cDC frequencies. **E)** Chemokine release assays of PBMC from healthy donors showed significantly elevated CXCL10 levels after 24h in-vitro PBMC exposure to CpG-B. F) At 48h, $CD14^+$ and $CD14^-CD11c^+$ (i.e. enriched for cDC1 cells) were sorted from the CpG-exposed PBMC cultures and put in culture separately. Supernatants were collected after overnight culture and both were found to contain equally high levels of CXCL10. Statistical significance: *, $P < 0.05$; **, $P < 0.01$; ***, $P < 0.001$.

Discussion

In this study we have shown that intradermal injection of CpG-B at the primary melanoma excision site results in an immune reaction in the skin that is still observed one week after administration (time of the re-excision). In a previous study, we found that the i.d. injection of GM-CSF in early stage melanoma patients resulted in an accumulation of $CD1a^{+}CD83^{+}$ DC in the papillary dermis, that correlated to $CD1a^{+}CD83^{+}$ migratory DC rates in matching SLN (23). In contrast, the injection of CpG-B did not induce migration of LC and dermal DC, which was in keeping of our previous finding that the migratory DC rates were not elevated in CpG-conditioned SLN (11,15). Rather, various DC/APC subsets were attracted primarily to the reticular dermis.

Consistent with a previous report from Haining and colleagues, we found an accumulation of pDC in the reticular dermis upon CpG ODN injection, that were mostly immature (24). In normal steady-state skin pDC are very rare, but the presence of immature pDC has been reported in the skin of patients with primary melanoma (25). pDC can also be recruited to the skin under inflammatory conditions as in cutaneous lupus erythematosus or psoriasis (26,27). Since both patient groups underwent a primary melanoma excision, often many weeks before the experimental treatment and re-excision, it is very likely that the skin at the primary excision site returned to steady-state. This is in line with our finding of nearly absent pDC in the dermis of patients in the saline control group. We previously described significantly higher activation and maturation states of pDC (by CD83, CD86 and CD40) in SLN of these same patients, most likely as a result of direct TLR9 stimulation with CpG-B (11). In our re-excision specimens however, we did not find CD83 co-expression on pDC. We hypothesize that the accumulation of these immature pDC in the re-excision specimens of patients that were treated with CpG-B is likely mediated by chemerin. Chemerin is a chemoattractant for cells that express CMKLR1 (chemokine-like receptor 1) which include circulating immature pDC (but not cDC) (28) and macrophages (29). Chemerin is expressed as an inactive pro-peptide in endothelial cells and fibroblasts in the healthy skin but can be activated upon skin injury (30) and bacterial infection (31) resulting in the accumulation of amongst others immature pDC ($BDCA2^{+}CD123^{+}$) and macrophages ($CD68^{+}$), as we have found in the skin of the CpG-B treated patients in our study. Remarkably, we previously did not find any increases in pDC rates in the SLN upon CpG-B delivery (11,15), further supporting the notion of a selective role for a skin-

restricted pDC chemoattractant, like chemerin. Of note, the local increase of pDC at the injection site provides a good rationale for repeated CpG-B administrations as their effects may be further amplified by direct activation and subsequent IFN-I release upon repeated CpG-B administration.

We found that the higher numbers of $CD83^+$ cells that were observed in the reticular dermis of patients who were injected with CpG-B were not pDC but CLEC9A expressing $CD141^+$ DC. These so-called cDC1 have been recognized as powerful (cross-)primers of cytotoxic T lymphocytes (CTL). $CD141^+$ cDC1 are known to express relatively high levels of CD83 and to originate from $CD141^+$ blood cDC1 that can be recruited to effector sites like the SLN and the skin in an IFNα dependent manner, as we previously described in patients who were treated with CpG-B with or without GM-CSF (15) . In mouse models, endogenous type IFN-I induced the accumulation of $CD8\alpha^+$ cDC1 (the murine equivalent of human $CD141^+$ cDC1) which was shown to be essential for spontaneous CTL priming against tumor antigens (32). Indeed, cDC1 in the TME and vaccine injection sites have been shown to migrate to draining lymph nodes and to induce CTL responses there (33,34). Moreover, more recent studies have demonstrated the importance of $CD103^+$ cDC1 in the release of CXCL10/CXCL9 and the subsequent attraction of effector T cells to the melanoma TME (19,20). These previous observations from mostly murine studies are in keeping with our findings from clinical specimens, showing clear correlations between CpG-induced IFN-I responses, cDC1 activation and recruitment to skin and SLN, CXCL10 expression, and T cell infiltration rates.

Besides cDC1, we also observed a significant increase in $CD14^+$ cell numbers in the CpG-injected skin, similar to what we previously described in lymph nodes, where $CD14^+$ and $CD141^+$ LNR-cDC were found to be present in higher numbers and activation states upon CpG-B treatment (13). We designated the CD14+ APC in the SLN as LNR-cDC, rather than macrophages, based on their (low) expression levels of CD83 and their ability to prime allogeneic T cells (12). Although we were unable to prove this for the $CD14^+$ APC in the re-excision specimens, we did find that the frequencies of $CD14^+$ LNR-cDC positively correlated with the number of $CD14^+$ APC in the reticular dermis, suggestive of co-recruitment upon i.d. CpG-B delivery. Flowcytometric analysis upon *in vitro* exposure to CpG-B showed activated monocytes to acquire an inflammatory $CD16^+$ phenotype with low levels of CD83 and elevated high levels of CD80 and PD-L1, suggestive of their T cell-activating capacity. Whereas in SLN

we found the $CD14^+$ APC to express CLEC9A, in the PBMC cultures we found them to be devoid of CLEC9A , which was consistent with our IHC findings in the skin re-excision samples, where CLEC9A was found to be co-expressed with CD141 and CD83, consistent with a mature cDC1 phenotype. This also is consistent with our findings in the PBMC cultures, showing CpG-induced elevation of levels of co-expressed CLEC9A, CD103, and CD83 on $CD141^+$ cDC1.

Whereas a previous study also identified $CD123^+$ pDC surrounded by T cells in the dermis of CpG-injected vaccination sites and in demonstrated an ability of pDC to attract T cells *in vitro*, our findings clearly suggest that the more numerous cDC1 and $CD14^+$ APC infiltrate in the reticular dermis is more vital to the subsequent recruitment of T cells. Indeed, we have observed high T cell infiltration rates upon i.d. administration of CpG-B in reticular dermis that was entirely devoid of pDC (see Figure 6C). Transcriptional data and data from *in-vitro* cultures indicate an important role for CXCL10 in this regard, with CXL10 production confirmed *in vitro* for both CD14+ APC and cDC1. To further confirm this in our skin-re-excision sites would require an extended multi-parameter IHC panel, possibly combined with CXCL10 mRNA *in situ* hybridization, which should be pursued in future studies.

As a T cell-inflamed microenvironment was shown to be beneficial in the context of melanoma vaccines and immune checkpoint inhibitors (35,36), we deem i.d. or intratumoral delivery of CpG ODN an important adjuvant therapy option in support of other immunotherapy approaches. While earlier murine studies delivered proof of this concept (37,38) a recent study from Ribas and colleagues on the combination of i.t. CpG administration and systemic PD-1 blockade confirmed this notion clinically (39). Our own findings in early-stage melanoma further indicate the clinical efficacy of CpG ODN as monotherapy, locally delivered at the primary tumor excision scar, in clinical stage I-II in a bid to overcome early LNR-cDC suppression in the draining lymph nodes. Indeed, Liang and colleagues showed that CpG can help overcome melanoma-related and β-catenin mediated suppression of DC (38).

In conclusion, our findings shed light on events following local CpG-B delivery, which lead to loco-regional recruitment of APC subsets and T cell infiltration and lead us to propose a model as presented in Supplementary Figure 4. I.d. injection of CpG-B triggers pDC activation and IFN-I release in the draining LN, which induces activation and subsequent recruitment of blood-borne cDC1 and monocytic precursors, both to the SLN and the skin injection site

(Supplementary Figure 4A). pDC attraction to the skin, but not to the SLN, may be related to dermal stroma-derived chemoattractants, such as chemerin. Of note, it is conceivable that such chemoattractants, locally induced by the direct activity of CpG-B, may be responsible for the initial recruitment of relatively small numbers of pDC and CD14+ APC, which may then trigger the subsequent recruitment of more numerous cDC1/CD14+ APC and T cells. Mature cDC1 from the reticular dermis may migrate to the SLN, carrying antigens, and may, in concert with $CD14^-$ and $CD14^+$ LNR-cDC, prime and/or boost melanoma-specific effector T cells, which upon recirculation through the blood, are attracted to effector sites (including the CpG-B injection site) by CXCL10, released predominantly by locally recruited cDC1 and $CD14^+$ APC (Supplementary Figure 4B). Locally delivered CpG ODN can thus contribute to the enhanced efficacy of systemic antitumor T cell responses, both in the induction and the effector phase.

Acknowledgments

The authors would like to thank Dr Joost Oudejans for pathological assessments and Coley Pharmaceutical Group for kind provision of CPG7909.

REFERENCES

1. Kashem SW, Haniffa M, Kaplan DH. Antigen-Presenting Cells in the Skin. Annu Rev Immunol. 2017;35:469–99.

2. Haniffa M, Shin A, Bigley V, McGovern N, Teo P, See P, et al. Human Tissues Contain CD141hi Cross-Presenting Dendritic Cells with Functional Homology to Mouse CD103^{+} Nonlymphoid Dendritic Cells. Immunity. 2012;37:60–73.

3. McGovern N, Schlitzer A, Gunawan M, Jardine L, Shin A, Poyner E, et al. Human Dermal CD14^{+} Cells Are a Transient Population of Monocyte-Derived Macrophages. Immunity. 2014;41:465–77.

4. Wollenberg A, Günther S, Moderer M, Wetzel S, Wagner M, Towarowski A, et al. Plasmacytoid Dendritic Cells: A New Cutaneous Dendritic Cell Subset with Distinct Role in Inflammatory Skin Diseases. J Invest Dermatol. 2002;119:1096–102.

5. Moseman EA, Liang X, Dawson AJ, Panoskaltsis-Mortari A, Krieg AM, Liu Y-J, et al. Human Plasmacytoid Dendritic Cells Activated by CpG Oligodeoxynucleotides Induce the Generation of CD4^{+}CD25^{+} Regulatory T Cells. J Immunol. 2004;173:4433–42.

6. Munn DH, Mellor AL. The tumor-draining lymph node as an immune-privileged site. Immunol Rev. 2006;213:146–58.

7. van den Hout MFCM, Koster BD, Sluijter BJR, Molenkamp BG, van de Ven R, van den Eertwegh AJM, et al. Melanoma Sequentially Suppresses Different DC Subsets in the Sentinel Lymph Node, Affecting Disease Spread and Recurrence. Cancer Immunol Res. 2017;5:969–77.

8. Krug A, Towarowski A, Britsch S, Rothenfusser S, Hornung V, Bals R, et al. Toll-like receptor expression reveals CpG DNA as a unique microbial stimulus for plasmacytoid dendritic cells which synergizes with CD40 ligand to induce high amounts of IL-12. Eur J Immunol. 2001;31:3026–37.

9. Krieg AM. CpG Motifs in Bacterial DNA and Their Immune Effects. Annu Rev Immunol. 2002;20:709–60.

10. Rothenfusser S, Tuma E, Endres S, Hartmann G. Plasmacytoid dendritic cells: the key to CpG. Hum Immunol. 2002;63:1111–9.

11. Molenkamp BG, van Leeuwen PAM, Meijer S, Sluijter BJR, Wijnands PGJTB, Baars A, et al. Intradermal CpG-B activates both plasmacytoid and myeloid dendritic cells in the sentinel lymph node of melanoma patients. Clin Cancer Res. 2007;13:2961–9.

12. Molenkamp BG, Sluijter BJR, van Leeuwen PAM, Santegoets SJAM, Meijer S, Wijnands PGJTB, et al. Local administration of PF-3512676 CpG-B instigates tumor-specific CD8^{+} T-cell reactivity in melanoma

patients. Clin Cancer Res. 2008;14:4532–42.

13. Koster BD, van den Hout MFCM, Sluijter BJR, Molenkamp BG, Vuylsteke RJCLM, Baars A, et al. Local Adjuvant Treatment with Low-Dose CpG-B Offers Durable Protection against Disease Recurrence in Clinical Stage I-II Melanoma: Data from Two Randomized Phase II Trials. Clin Cancer Res. United States; 2017;23:5679–86.

14. Vuylsteke RJCLM, Molenkamp BG, Gietema HA, van Leeuwen PAM, Wijnands PGJTB, Vos W, et al. Local Administration of Granulocyte/Macrophage Colony-stimulating Factor Increases the Number and Activation State of Dendritic Cells in the Sentinel Lymph Node of Early-Stage Melanoma. Cancer Res. 2004;64:8456–60.

15. Sluijter BJR, van den Hout MFCM, Koster BD, van Leeuwen PAM, Schneiders FL, van de Ven R, et al. Arming the Melanoma Sentinel Lymph Node through Local Administration of CpG-B and GM-CSF: Recruitment and Activation of BDCA3/CD141^{+} Dendritic Cells and Enhanced Cross-Presentation. Cancer Immunol Res. 2015;3:495–505.

16. van de Ven R, van den Hout MFCM, Lindenberg JJ, Sluijter BJR, van Leeuwen PAM, Lougheed SM, et al. Characterization of four conventional dendritic cell subsets in human skin-draining lymph nodes in relation to T-cell activation. Blood. 2011;118:2502–10.

17. Koster BD, de Jong TD, van den Hout MFCM, Sluijter BJR, Vuylsteke RJCLM, Molenkamp BG, et al. In the mix: the potential benefits of adding GM-CSF to CpG-B in the local treatment of patients with early-stage melanoma. Oncoimmunology. 2020;9:1708066.

18. Pfirschke C, Siwicki M, Liao H-W, Pittet MJ. Tumor Microenvironment: No Effector T Cells without Dendritic Cells. Cancer Cell. 2017;31:614–5.

19. Spranger S, Dai D, Horton B, Gajewski TF. Tumor-Residing Batf3 Dendritic Cells Are Required for Effector T Cell Trafficking and Adoptive T Cell Therapy. Cancer Cell. 2017;31:711-723.e4.

20. Chow MT, Ozga AJ, Servis RL, Frederick DT, Lo JA, Fisher DE, et al. Intratumoral Activity of the CXCR3 Chemokine System Is Required for the Efficacy of Anti-PD-1 Therapy. Immunity. 2019;50:1498-1512.e5.

21. Broz ML, Binnewies M, Boldajipour B, Nelson AE, Pollack JL, Erle DJ, et al. Dissecting the Tumor Myeloid Compartment Reveals Rare Activating Antigen-Presenting Cells Critical for T Cell Immunity. Cancer Cell. 2014;26:638–52.

22. Sichien D, Scott CL, Martens L, Vanderkerken M, Van Gassen S, Plantinga M, et al. IRF8 Transcription Factor Controls Survival and Function of Terminally Differentiated Conventional and Plasmacytoid Dendritic Cells, Respectively. Immunity. 2016;45:626–40.

23. Molenkamp BG, Vuylsteke RJCLM, van Leeuwen PAM, Meijer S, Vos W, Wijnands PGJTB, et al. Matched

Skin and Sentinel Lymph Node Samples of Melanoma Patients Reveal Exclusive Migration of Mature Dendritic Cells. Am J Pathol. 2005;167:1301–7.

24. Haining WN, Davies J, Kanzler H, Drury L, Brenn T, Evans J, et al. CpG Oligodeoxynucleotides Alter Lymphocyte and Dendritic Cell Trafficking in Humans. Clin Cancer Res. 2008;14:5626–34.

25. Vermi W, Bonecchi R, Facchetti F, Bianchi D, Sozzani S, Festa S, et al. Recruitment of immature plasmacytoid dendritic cells (plasmacytoid monocytes) and myeloid dendritic cells in primary cutaneous melanomas. J Pathol. John Wiley & Sons, Ltd.; 2003;200:255–68.

26. Farkas L, Beiske K, Lund-Johansen F, Brandtzaeg P, Jahnsen FL. Plasmacytoid dendritic cells (natural interferon- alpha/beta-producing cells) accumulate in cutaneous lupus erythematosus lesions. Am J Pathol. American Society for Investigative Pathology; 2001;159:237–43.

27. Nestle FO, Conrad C, Tun-Kyi A, Homey B, Gombert M, Boyman O, et al. Plasmacytoid predendritic cells initiate psoriasis through interferon-α production. J Exp Med. 2005;202:135–43.

28. Zabel BA, Silverio AM, Butcher EC. Chemokine-like receptor 1 expression and chemerin-directed chemotaxis distinguish plasmacytoid from myeloid dendritic cells in human blood. J Immunol. 2005;174:244–51.

29. Zabel BA, Ohyama T, Zuniga L, Kim JY, Johnston B, Allen SJ, et al. Chemokine-like receptor 1 expression by macrophages in vivo: Regulation by TGF-β and TLR ligands. Exp Hematol. 2006;34:1106–14.

30. Gregorio J, Meller S, Conrad C, Di Nardo A, Homey B, Lauerma A, et al. Plasmacytoid dendritic cells sense skin injury and promote wound healing through type i interferons. J Exp Med. 2010;207:2921–30.

31. Kulig P, Zabel BA, Dubin G, Allen SJ, Ohyama T, Potempa J, et al. Staphylococcus aureus -Derived Staphopain B, a Potent Cysteine Protease Activator of Plasma Chemerin. J Immunol. 2007;178:3713–20.

32. Fuertes MB, Kacha AK, Kline J, Woo SR, Kranz DM, Murphy KM, et al. Host type I IFN signals are required for antitumor $CD8^+$ T cell responses through $CD8\alpha^+$ dendritic cells. J Exp Med. 2011;208:2005–16.

33. Roberts EW, Broz ML, Binnewies M, Headley MB, Nelson AE, Wolf DM, et al. Critical Role for $CD103^+$ /$CD141^+$ Dendritic Cells Bearing CCR7 for Tumor Antigen Trafficking and Priming of T Cell Immunity in Melanoma. Cancer Cell. 2016;30:324–36.

34. Bąbała N, Bovens A, de Vries E, Iglesias-Guimarais V, Ahrends T, Krummel MF, et al. Subcellular Localization of Antigen in Keratinocytes Dictates Delivery of $CD4^+$ T-cell Help for the CTL Response upon Therapeutic DNA Vaccination into the Skin. Cancer Immunol Res. 2018;6:835–47.

35. Ji R-R, Chasalow SD, Wang L, Hamid O, Schmidt H, Cogswell J, et al. An immune-active tumor microenvironment favors clinical response to ipilimumab. Cancer Immunol Immunother.

2012;61:1019–31.

36. Gajewski TF, Louahed J, Brichard VG. Gene signature in melanoma associated with clinical activity: a potential clue to unlock cancer immunotherapy. Cancer J. 2010;16:399–403.

37. Reilley MJ, Morrow B, Ager CR, Liu A, Hong DS, Curran MA. TLR9 activation cooperates with T cell checkpoint blockade to regress poorly immunogenic melanoma. J Immunother Cancer. 2019;7:323.

38. Liang X, Fu C, Cui W, Ober-Blöbaum JL, Zahner SP, Shrikant PA, et al. β-catenin mediates tumor-induced immunosuppression by inhibiting cross-priming of $CD8^+$ T cells. J Leukoc Biol. 2014;95:179–90.

39. Ribas A, Medina T, Kummar S, Amin A, Kalbasi A, Drabick JJ, et al. SD-101 in Combination with Pembrolizumab in Advanced Melanoma: Results of a Phase Ib, Multicenter Study. Cancer Discov. 2018;8:1250–7.

SUPPLEMENTARY MATERIALS

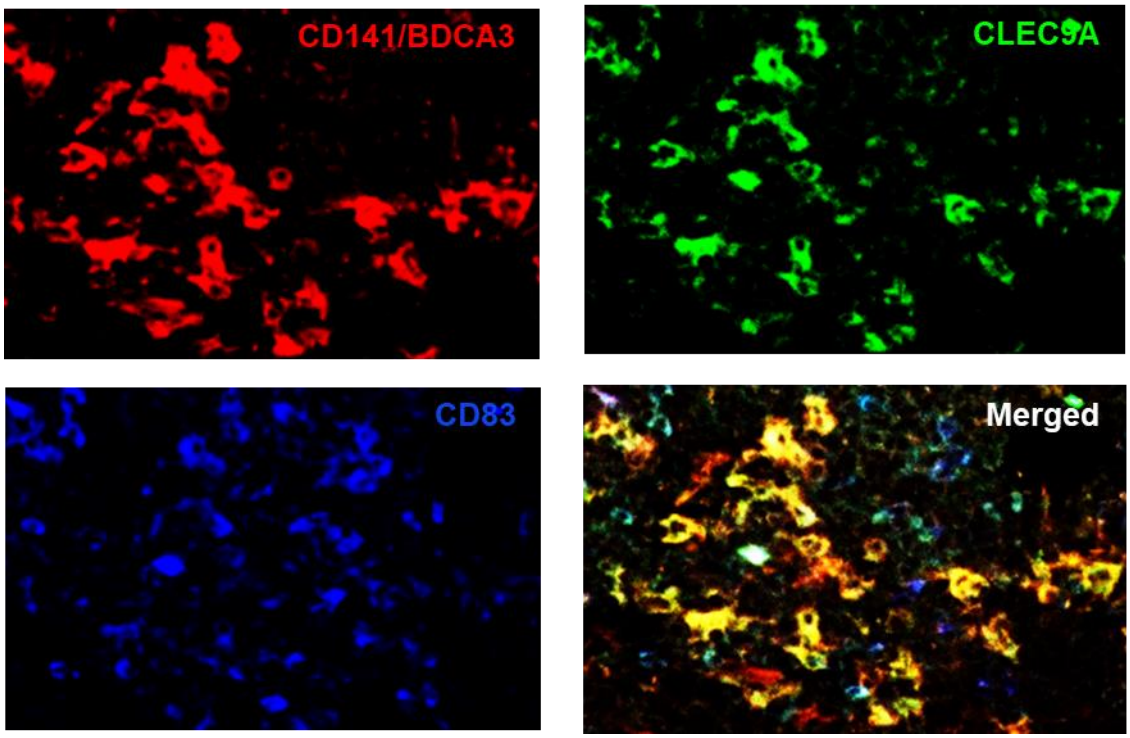

Supplementary Figure 1. cDC1 in tonsil tissue

A representative positive control example a CD83/CD141/CLEC9A triple fluorescent IHC stain on a tonsil section

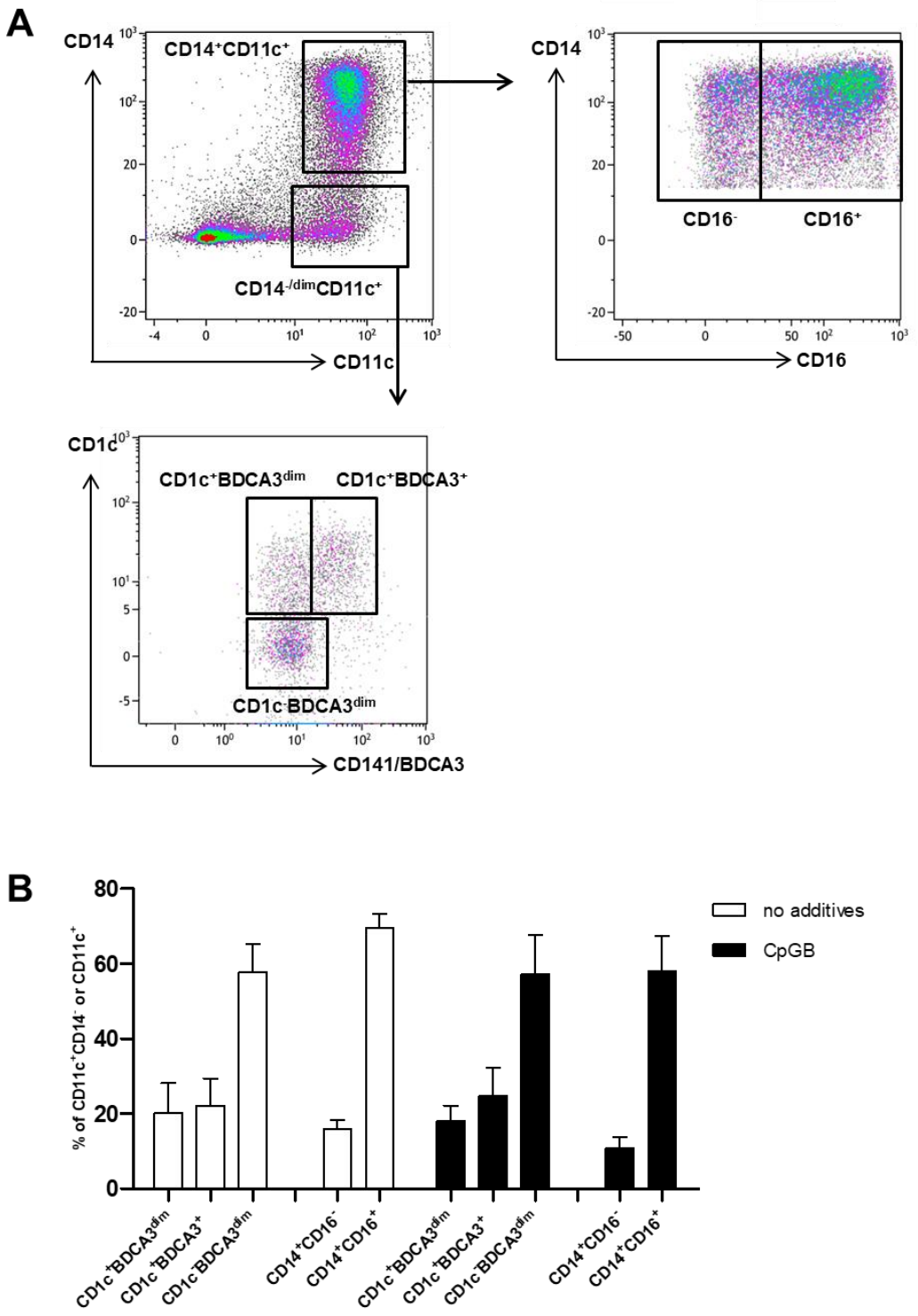

Supplementary Figure 2. Myeloid APC subsets in CpG-B exposed cultures of peripheral blood mononuclear cells (PBMC)

A) Gating strategies for myeloid cDC and monocytic APC subsets from *in vitro* PBMC cultures, and **B)** their distribution in the control and CpG-B cultures (48h).

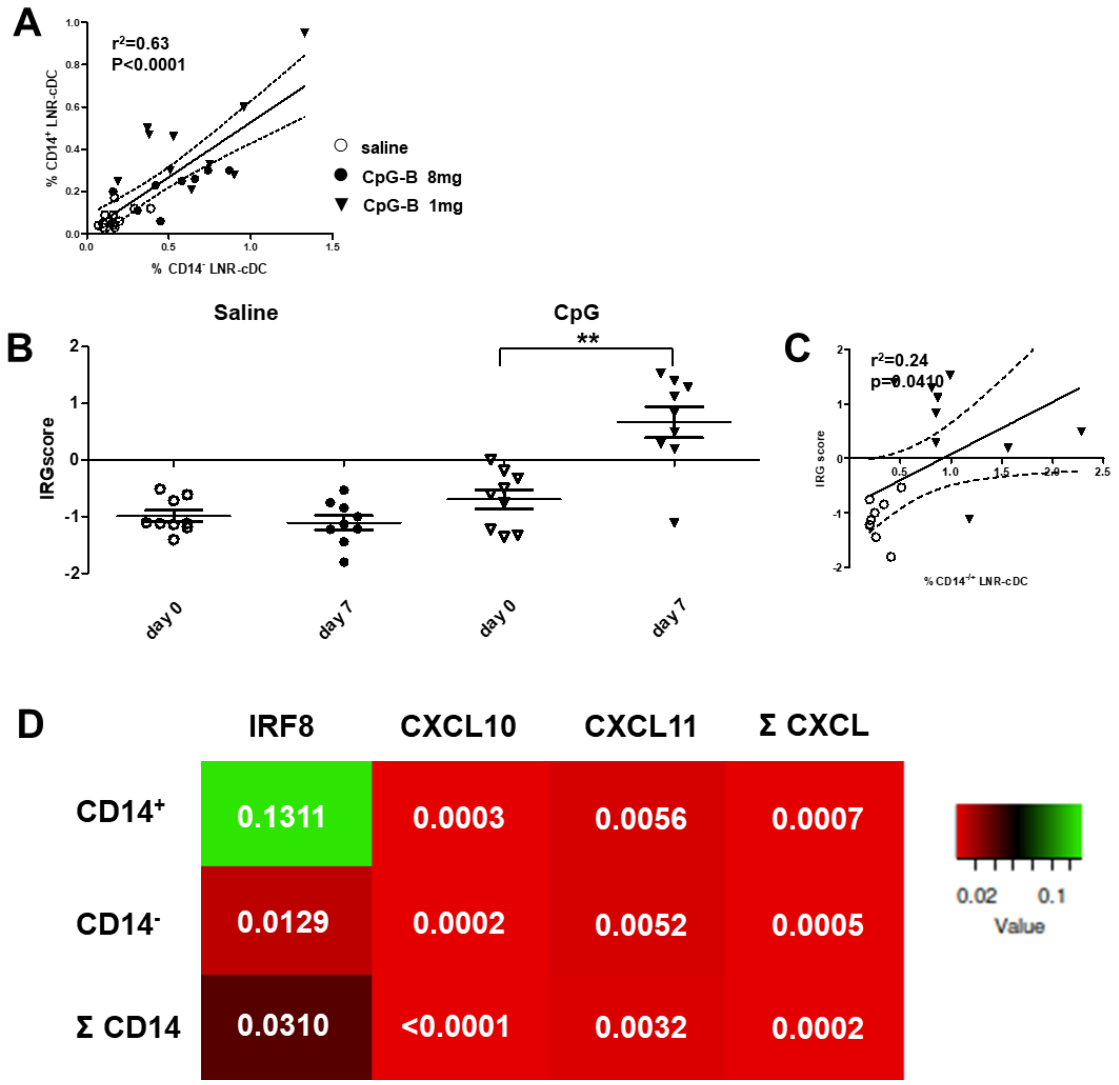

Supplementary Figure 3. Lymph node resident (LNR) cDC subsets in relation to a CpG-B induced type-1 IFN (IFN-I) response signature

A) We found similar co-recruitment of $CD14^-$ and $CD14^+$ LNR-cDC/APC to the SLN at different dose levels of CpG-B (1 and 8 mg) in two separate trials. **B)** Transcriptional analysis of 47 known IFN-I response genes (IRG) showed that there was a significant induction of an IFN-I response in PBMC at 7 days after the first i.d. injection of 1mg CpG-B. **C)** IRG score correlated significantly with the $CD14^-$ and $CD14^+$ LNR-cDC rates in SLN. **D)** Heat map of Pearson correlation P values for the IRF8 and the separate or combined CXCL10 and CXCL11 transcript levels versus the separate or combined $CD14^-$ and $CD14^+$ cDC rates in the SLN. Heat map constructed in heatmapper.ca.

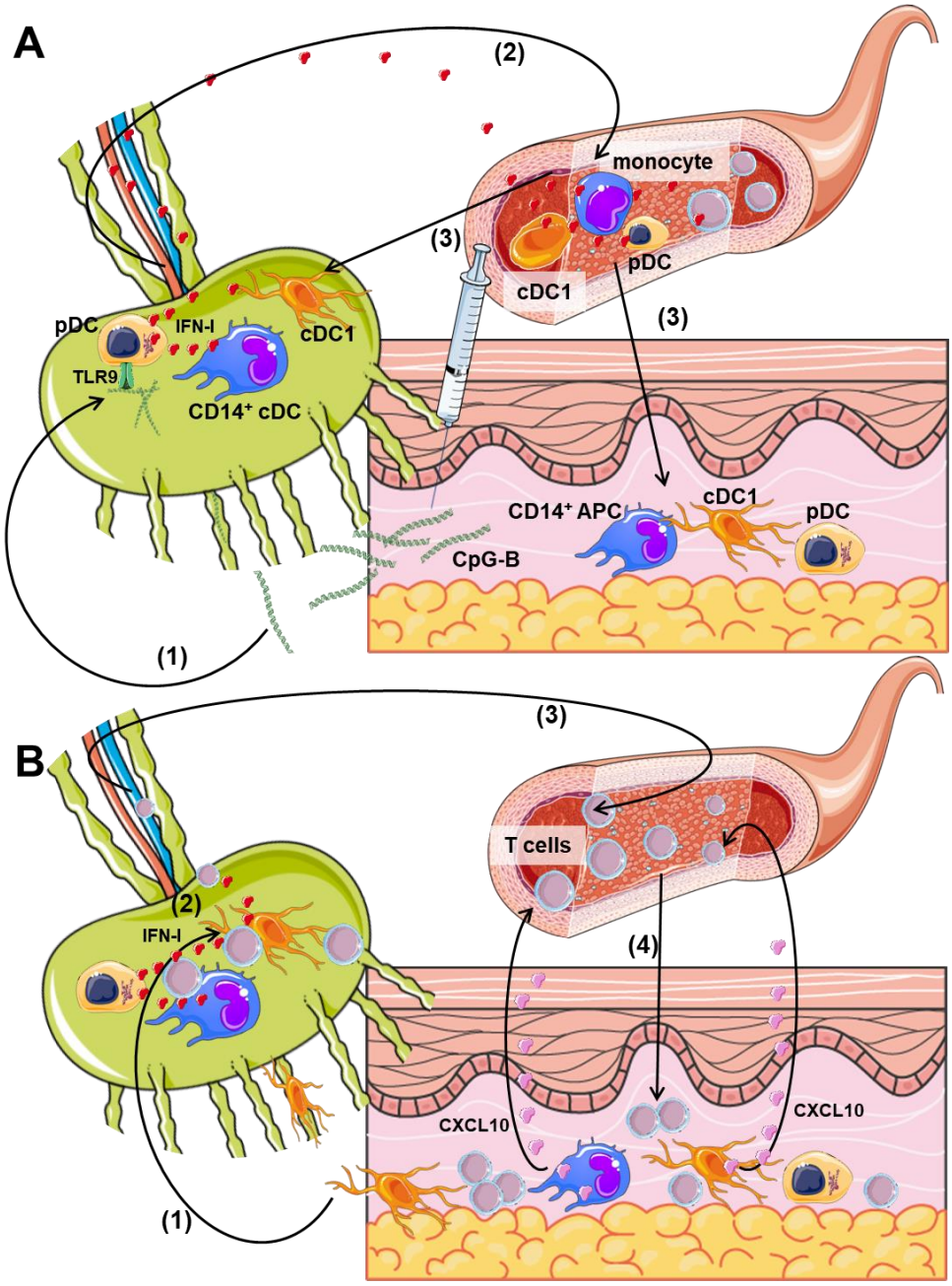

Supplementary Figure 4. A model of CpG-B-induced APC and T cell trafficking.

A) Intradermal injection of CpG-B triggers (1) pDC activation and IFN-I release in the draining LN, which induces (2) activation and (3) subsequent recruitment of blood-borne cDC1 and monocytic precursors, both to the SLN and the skin injection site (Supplementary Figure 4A). pDC attraction to the skin, but not to the SLN, may be related to dermal stroma-derived chemoattractants, such as chemerin. **B)** (1) Mature cDC1 from the reticular dermis may migrate to the SLN, carrying antigens, and (2) may, in concert with $CD14^-$ and $CD14^+$ LNR-cDC, prime and/or boost melanoma-specific effector T cells, which (3) upon recirculation through the blood, (4) are attracted to effector sites (including the CpG-B injection site) by CXCL10, released predominantly by locally recruited cDC1 and $CD14^+$ APC.